ELSEVIER

Journal of Hazardous Materials 76 (2000) 301–337

Journal of Hazardous Materials

www.elsevier.nl/locate/jhazmat

Effective use of fly ash slurry as fill material

Sumio Horiuchi [a,*], Masato Kawaguchi [a,1], Kazuya Yasuhara [b,2]

[a] *Institute of Technology, Shimizu Corporation, 3-4-17 Etchujima, Koto-ku, Tokyo 135-8530 Japan*
[b] *Department of Civil Engineering, Ibaraki University, Ibaraki, Japan*

Received 29 March 1999; received in revised form 15 January 2000; accepted 26 February 2000

Abstract

A lot of effort has been put into increasing coal ash utilization; however, 50% of total amount is disposed of on land and in the sea. Several attempts have been reported recently concerning slurried coal fly ash use for civil engineering materials, such as for structural fill and backfill. The authors have studied this issue for more than 15 years and reported its potential for (1) underwater fills, (2) light weight backfills, and (3) light weight structural fills, through both laboratory tests and construction works. This paper is an overview of the results obtained for slurry, focusing on the following. (1) Coal fly ash reclaimed by slurry placement shows lower compressibility, higher ground density, and higher strength than by the other methods. This higher strength increases stability against liquefaction during earthquake. (2) Higher stability of the fly ash ground formed by slurry placement is caused by higher density and its self-hardening property. (3) Stability of fly ash reclaimed ground can be increased by increasing density and also by strength enhancement by cement addition. (4) Technical data obtained through a man-made island construction project shows the advantages of fly ash slurry in terms of mechanical properties such as higher stability against sliding failure, sufficient ground strength, and also in terms of cost saving. (5) Concentration in leachates from the placed slurry is lower than the Japanese environmental law. (6) In order to enlarge the fly ash slurry application toward a lightweight fill, mixtures of air foam, cement and fly ash were examined. Test results shows sufficient durability of this material against creep failure. This material was then used as lightweight structural fill around a high-rise building, and

* Corresponding author. Tel.: +81-3-3820-5519; fax: +81-3-3820-5955.
E-mail addresses: horiuchi@sit.shimz.co.jp (S. Horiuchi), masando@sit.shimz.co.jp (M. Kawaguchi), yasuhara@civil.ibaraki.ac.jp (K. Yasuhara).
[1] Tel.: +81-3-3820-5519; fax: +81-3-3820-5955.
[2] Tel.: +81-294-35-6101; fax: +81-294-35-8146.

PII: S0304-3894(00)00205-3

showed sufficient quality. From the above data, it can be concluded that coal fly ash slurry can be effectively utilized in civil engineering projects.

Keywords: Coal fly ash; Slurry; Reclamation; Fill; Strength

1. Introduction

More than 7 Tg (10^{12} g) of coal ash are discharged from power plants in Japan, and are utilized in various fields such as a raw material in the cement industry, concrete additives, and road materials. The utilization rate is around 50%, and the rest is disposed of in the sea and on land. Seventy percent of total utilization is covered in the cement industry, in which a large increase in utilization is not expected in the future because of limits to acceptable quantity. Utilization as fill material, such as structural fill and back-fill, is expected to be the next main way because such projects require enormous quantity of coal ash.

Coal fly ash, the fine spherical particles which make up 80% of coal ash, has been used as an additive for mortar and concrete to improve fluidity. It is also used as the main component of slurries for grout [1,2]; however, a large amount of cement was mixed with the slurries to develop sufficient strength. For the fill, compressive strength of 1 MPa is adequate; however, few studies have also been reported for materials of lower strength.

In Japan, sea disposal of the coal ash has increased because of the shortage of land disposal sites. The current problems associated with sea disposal are low strength and low density. If the density of coal ash slurry (flowable fill) is high enough, then underwater placement of the slurry, as shown Fig. 1, provides a new effective disposal system to increase both density and bearing capacity. The specifications of underwater placement, such as appropriate viscosity and density decrease during placement, are important for planning the system.

Underwater placement of the fly ash slurry is thought to be suitable for a stable artificial ground construction in big projects such as harbor or airport construction. Effect on strength development, such as temperature and additives, are major concern for preparing appropriate slurries. Evaluation of the mass properties is essential for

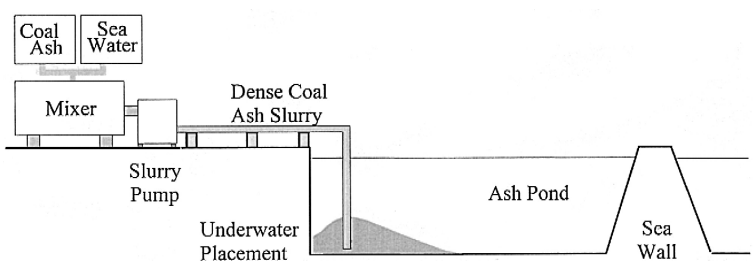

Fig. 1. Concept of slurry reclamation.

design. The mechanical and environmental stability of the placed slurry are also quite important in such utilization.

One of the latest geo-materials is lightweight fill. Foamed mortar is one such material; however, it is too strong and is subject to temperature increases caused by cement hydration. Since the fly ash has a high pozzolanic activity and a low specific gravity, it was expected that fly ash could be a partial substitute for cement in foamed mortar. The properties of the material necessary for construction design, such as strength development, cohesion and frictional angle, and creep.

The authors have studied fly ash slurries as possible fill materials [3–11], because almost all the points described above had not been reported. Coal fly ash is not considered a hazardous waste; however, the data collected could be applied for other waste materials.

In this paper, the following three issues in our studies are reviewed.

1. Effective fly ash disposal using high density slurry
2. Man-made island construction using fly ash slurry
3. Lightweight slurry for structural fill.

2. Underwater disposal using fly ash slurry

2.1. Outline

Sea disposal of coal ash has increased in Japan, because of insufficient disposal land near the power plants that produce it. The major concern now is how to increase the density of coal ash disposed underwater. Conventional sea disposal is classified into two types: wet disposal and dry disposal. In wet disposal, coal ash is sluiced into the sea, i.e. coal ash is mixed with a large amount of seawater and is hydraulically transported through pipelines to the disposal site. In dry disposal, coal ash conditioned with water is transported with belt conveyors or dump trucks to the shore, and dumped into the sea. Despite the importance of disposal capacity, density data for coal ash disposed of underwater has been limited and vague [12–15]. According to a recent report [7] the dry density by the wet reclamation at accumulation speed of 10 cm/day is 46–58% of the maximum dry density determined by the standard Proctor test (ASTM D698-91, Procedure A), and the shear strength of the ground is less than 20 kPa.

It was expected that the fly ash slurry would show a higher density than the wet reclamation, and the underwater placement of the slurry would provide a new effective disposal system to increase both density and bearing capacity. In this section, studies carried out to confirm the advantages of this new disposal method are reviewed.

2.2. Experiments

2.2.1. Materials

(1) Coal fly ash: more than 50 kinds of coal fly ash were used in this study. All the samples were collected from Japanese coal power plants and kept dry. Table 1 shows

Table 1
Properties of coal fly ash

Fly ash name		A	B	C	D	E	F	G	H	I	L	M	N	O	P	Q	R	V
Specific gravity		2.23	2.25	2.31	2.38	2.28	2.15	2.32	2.23	2.26	2.11	2.22	2.44	2.24	2.11	2.19	2.21	2.25
Mean diameter (μm)		41	17	11.5	9.7	7.8	23	14	11	12	18	19	9.2	13	18	10	12	17
Max. dry density (g/cm^3)[a]		1.37	1.36	1.47	1.42	1.25	1.24	1.16	1.07	1.10	1.24	1.30	1.33	1.15	1.24	–	–	1.46
Opt. water content (%)[a]		20.3	21.0	17.2	20.5	24.0	24.8	32.4	36.2	34.1	25.5	24.7	26.5	31.3	25.5	–	–	16.8
Ignition loss (%)		2.40	3.34	1.66	3.57	4.61	2.64	5.32	8.41	2.33	2.00	5.30	2.78	7.64	2.00	1.75	4.06	2.17
Initial pH		–	12.8	12.7	12.6	12.7	12.8	12.4	11.9	12.1	4.1	11.0	11.7	12.2	4.1	4.2	11.7	12.7
Chemical component (%)	SiO_2	53.0	53.5	51.0	50.3	56.6	61.0	58.8	49.1	64.6	66.2	58.5	49.4	49.2	60.0	76.4	65.9	49.7
	Al_2O_3	27.8	23.7	25.0	28.0	26.2	25.7	19.7	27.9	24.8	26.8	24.1	27.4	28.6	25.9	18.9	19.3	24.1
	Fe_2O_3	5.40	4.81	5.87	5.52	3.86	2.24	5.56	5.59	3.25	1.00	5.50	10.2	6.44	4.24	1.91	3.85	5.09
	CaO	7.60	7.28	9.12	6.12	3.40	3.82	6.01	3.18	1.62	0.80	2.50	3.98	2.25	2.42	0.14	2.71	9.97
	SO_3	0.40	0.33	0.40	0.73	0.39	0.14	0.75	0.38	0.32	–	–	0.92	0.34	0.42	–	–	0.36

[a] Standard Proctor test (ASTM D698-91, Procedure A).

chemical and physical properties of representative samples. Each chemical composition is shown as an oxide form of the element.

(2) Mixing and curing water: pH 8 artificial seawater and natural seawater were used for preparation and for curing the samples.

(3) Cement: Ordinary Portland Cement (OPC) was used for strength enhancement.

2.2.2. Procedures

Fly ash slurries were prepared by two different techniques, single mixing (SM) and double mixing (DM) as described in Fig. 2. The advantage of double mixing was discovered accidentally at the preliminary test stage. This testing was necessary to confirm the amount of water required for the flowable slurry; namely, coal ash slurries prepared by step-by-step water addition and mixing showed less viscosity than the single-mixing slurries. As a standard double mixing procedure, the ratio of the initial water to the total water (initial water ratio) was fixed at 67%.

A Hobert type mixer was used to prepare the slurries at a rotary speed of 140 rpm and a planetary speed of 60 rpm. The viscosity of the coal ash slurry was determined within 1 min after the preparation using 15 cm slump cone for plasters.

Samples for strength tests were prepared by pouring the slurry into plastic molds 5 cm in diameter and 10 cm in height. The samples in the molds covered by polyethylene film were immersed and cured in water at 20°C until the strength test. Strength was determined by a laboratory vane test or an unconfined compression test, followed by dry density measurement.

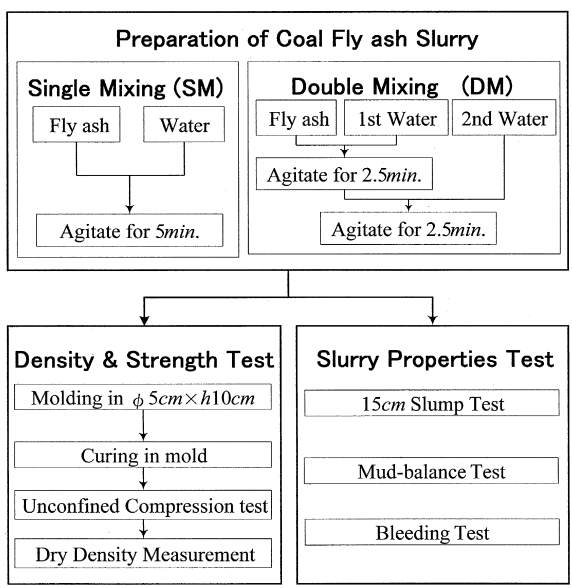

Fig. 2. Test flow of fly ash flurry.

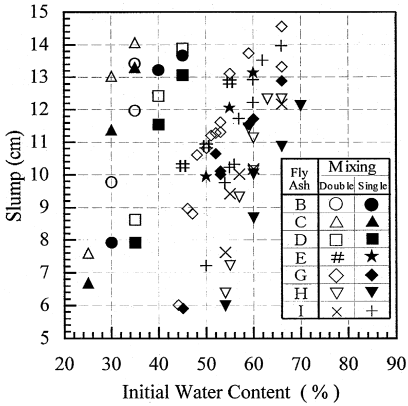

Fig. 3. Slurry slump and water content.

2.3. Results and discussions

2.3.1. Slurry viscosity and dry density

The viscosity of coal ash slurries are shown in Fig. 3, in which the slurry viscosity is decreased with water content increasing and differs greatly from the coal ash type. The double-mixing slurries show less viscosity than the single-mixing slurries; a higher slump is obtained by the double mixing at the same water content. This means that with the double mixing, a higher density slurry can be produced than with conventional methods.

A relationship between the slurry slump and the dry density of the hardened sample is shown in Fig. 4, where the dry densities of the slurries decrease with the increase in the slump. The effect of first water content on slump of the double-mixing slurry is shown in Fig. 5. The highest slump is obtained when the first water content is 40–45%, which correspond to 116–126% of the optimum water content. A higher slump was also

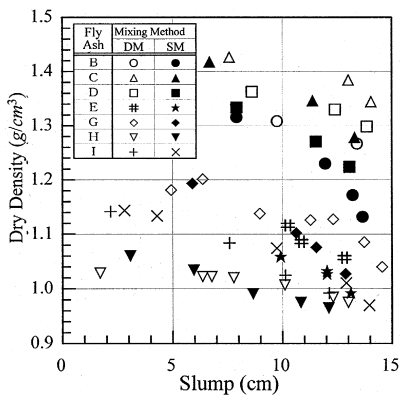

Fig. 4. Slurry density and slump.

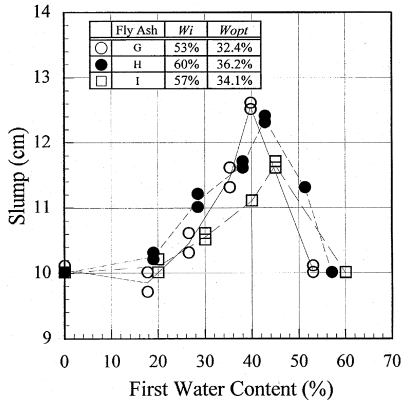

Fig. 5. Effect of first water on slump.

observed when the first mixing speed or first mixing period was increased. These phenomena suggest that the double mixing effect may be caused by the mechanical change of coal ash particles occurring during the first mixing. Since some technical papers have reported the particle degradation of coal ash during the compaction process [16,17], it would seem reasonable to conclude that some fractions in coal ash, such as large and irregular particles, are broken into pieces by a shear force exerted during the mixing, and that this change in size distribution may decrease voids in the slurry and increase its density. This particle degradation was confirmed through additional tests.

2.3.2. Strength development

Strength development of the slurries is shown in Fig. 6, where coal ashes B and D show a long-term strength development, similar to the compacted coal ashes [18,19]. ''*a*'' and ''*b*'' on the figure are constants of approximation formula of $qu = a(t)^b$,

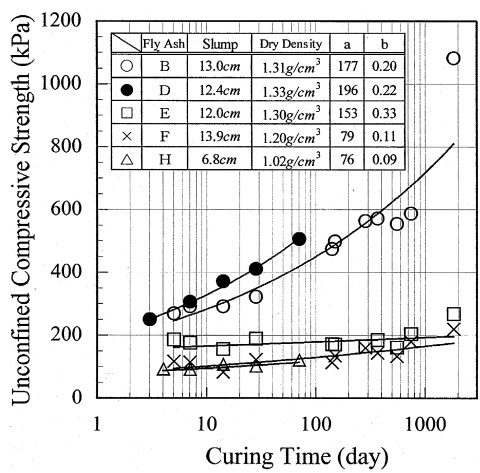

Fig. 6. Strength development of slurry.

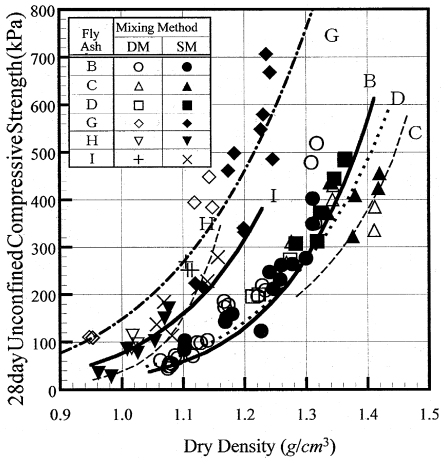

Fig. 7. Strength and dry density of slurry.

where qu is the unconfined compressive strength and t is the curing date. There is no discussion on the mechanism of strength development after two years of curing in the case of coal.

Fig. 7 shows the relationship between 28-day strength and density, in which qu can be approximately expressed with dry density (ρ_d) using the following equation; $qu = A(\rho_d)^B$, where both A and B are constant. Using these relationships, the strength of the underwater sample can be estimated.

Assuming unconfined compressive strength of 200 kPa is needed for actual land usage, the 1-year strengths of slurries E, F and H in Fig. 6 are not sufficient. Even though there remains a possibility of increasing their strengths in the future, it may be difficult to attain a sufficient strength in all kinds of coal ashes. To enhance and accelerate strength development, the addition of cement or gypsum would be easy and effective [4] with this slurry disposal system.

2.3.3. Underwater placement tests

The shape of the placed mass is important for planning the practical placing procedures, such as the pitch of placing points and the volume of each lift. The appropriate fluidity for underwater placement and homogeneity of the placed mass was not known. To investigate these points, underwater placing tests using a 6 m^3 test tank (110 cm height, 120 cm width and 470 cm length) were carried out. Table 2 shows the properties of slurries used in the 6 m^3 test tank underwater placing tests. Distribution of

Table 2
Specifications of underwater placing tests using 6 m^3 test tank

Test no.	Dry density (g/cm^3)	Compressive strength (MPa)	Slump (cm)
27	1.37	0.41	13.9
28	1.34	0.99	12.3
29	1.29	0.68	9.6

density and strength were determined more than 1 month after the placement. Compressive strength on Table 2 was determined at the same curing date as distribution measurement.

Fig. 8 shows shape and dry density distribution. The slurries were placed at 50 cm from the left side. The slope of placed slurry varies with the fluidity of the slurry; the lower the slump, the steeper the slope. Partial break down of the slope was observed when the slope exceeded 15°, and resulted in a decrease in both density and strength. For a slope of less than 5°, slurry can be placed without slope break down; however, it flows too fast and far, and it is difficult to place slurry without disturbance.

As seen in density distributions, except for the very surface of the three masses and the sediment from slope break down of test No. 29, the placed mass is uniform in density. The average dry densities of the three masses in Fig. 8 are 1.30 g/cm^3, 1.30 g/cm^3 and 1.25 g/cm^3, respectively. The density decrease caused by the disturbance or slope break down during the underwater placement is, therefore, 5.1%, 3.0%, and 3.1%. This density drop, however, could be expected to decrease with the increase in placing volume.

Fig. 9 shows strength distribution of the masses. Because strength is closely related to dry density, placed mass is also uniform in strength. Comparing Fig. 9 with Table 2, strength of the placed masses is higher than that of the mold samples. This tendency

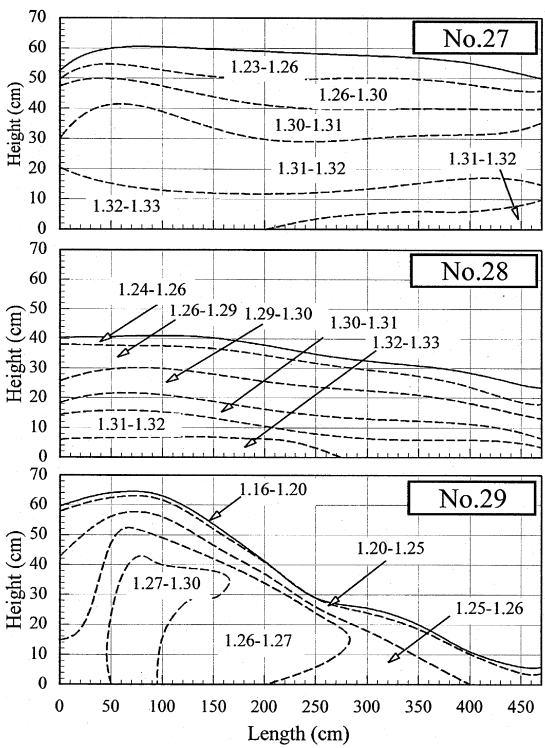

Fig. 8. Distribution of dry density of placed masses (g/cm^3).

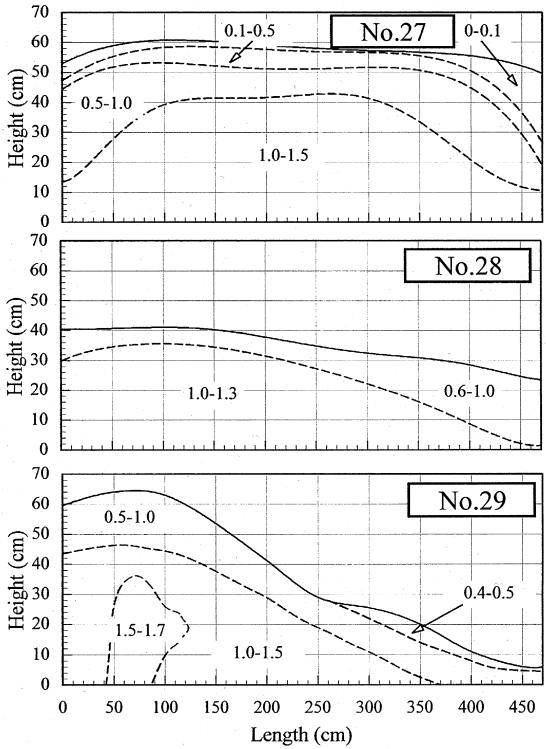

Fig. 9. Distribution of strength (MPa).

results from differences of such curing conditions as a higher curing temperature and higher confining pressure in the placed mass, and the presence of a soft upper part in the mold samples.

The relationship between the slope and the slump is shown in Fig. 10, in which past results obtained in smaller size underwater placing tests are also plotted. Since the slope

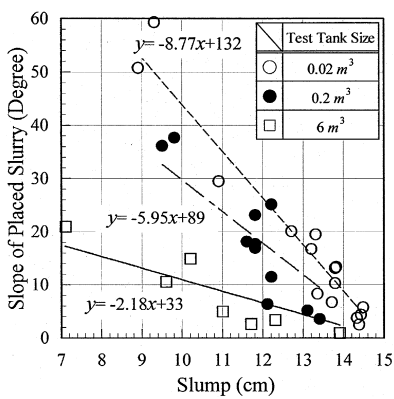

Fig. 10. Slope of the placed mass and slurry slump.

of the mass increases with decreasing test tank size as seen in Fig. 10, a full scale test is the ideal way to predict the actual slope. If we reclaim using a fly ash slurry placement conical shape of 200 m^3 with a 10° slope, the height of each would be 1.6 m. The 6 m^3 tank tests are, therefore, 1/2–1/4 of the actual size, and this scale test seems to be large enough for an accurate prediction.

From the placement tests, the appropriate slope can be determined as 5–10°, and therefore optimal slump for the actual underwater placement can be determined as 11 cm.

2.3.4. Evaluation of slurry reclamation

As the coal ash slurry should be placed under water, the density of the slurry has to be evaluated at a given viscosity suitable for the placement. As seen in Fig. 4, coal ash type affects density of its water mixture. To evaluate the slurry density, the density ratio (R_d: ratio of the dry density of the 11 cm slump slurry to the maximum dry density) is plotted against the mean diameter in Fig. 11. The mean diameter of the coal ash is 0.015 mm on average, so the average density ratio expected is 92% for the single mixing and 96% for the double mixing, respectively. The tendency in Fig. 11, in which R_d decreases with the decrease of the mean diameter, may be explained by the difficulty in degradation of smaller particles.

The density decrease during the placement would be less than 4%. Since the density ratio of the double-mixing slurry is 96%, the density ratio by the slurry reclamation can be expected to be more than 92%. This density is even higher than the field compaction made by six passes of a 10- to 12-ton tired roller [12].

In Fig. 12, the strength of a 11-cm slump slurry after 28 days is plotted against the calcium content. The relationship has a rather large scattering, and an increase in the calcium content results in an increase in the strength. Advantages of the slurry reclamation on static and dynamic properties are confirmed using a coal ash of 2.03% in calcium content [10]. It could be speculated that coal ash having more than 4% calcium content would develop unconfined compressive strength of 200 kPa or more, and would be sufficient for land uses.

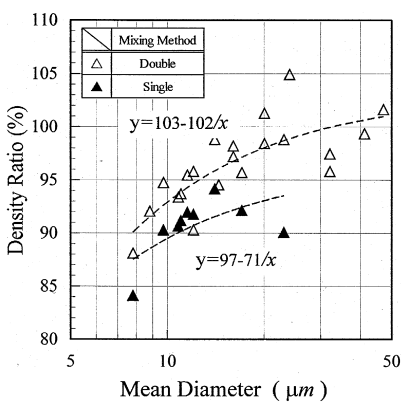

Fig. 11. Density ratio of fly ash slurries.

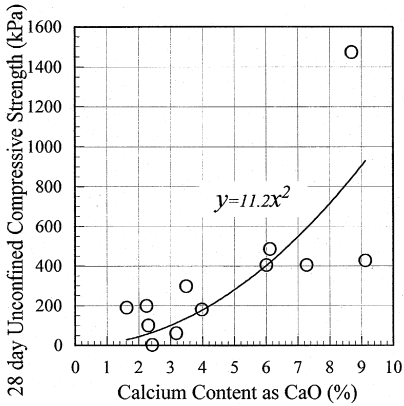

Fig. 12. Calcium content and slurry strength.

To obtain additional information of the placed fly ash mass, triaxial tests were carried out using a fly ash containing 2% calcium content. The stress path of a placed mass is shown in Fig. 13. Shear resistance of HAS (High-density Ash Slurry) increases along with the critical state line in both the compression and the tensile processes, like soils in a dense state, but the dry reclaimed sample shows a behavior resembleing a loose weak sandy soil. Inclinations of the critical state lines are slightly different, Me (inclination during the tensile process: broken line) is smaller than Mc (inclination during the compression process: solid line), and this is because of the anisotropic microstructure of the both placed masses.

Fig. 14 shows the number of cycles to reach 5% strain (DA = 5%) of both dry reclamation and slurry placement samples determined by undrained triaxial tests conducted at a loading frequency of 0.1 Hz under constant confined pressure of 0.098 MPa. The placed fly ash slurry mass shows a higher resistance against dynamic load than the Toyoura sand of 70% D_r, relative density. This means a higher resistance against

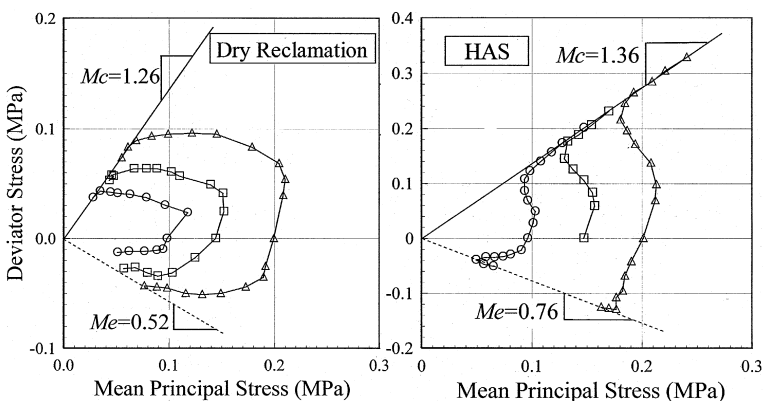

Fig. 13. Stress path of dry reclaimed mass and slurry reclaimed mass.

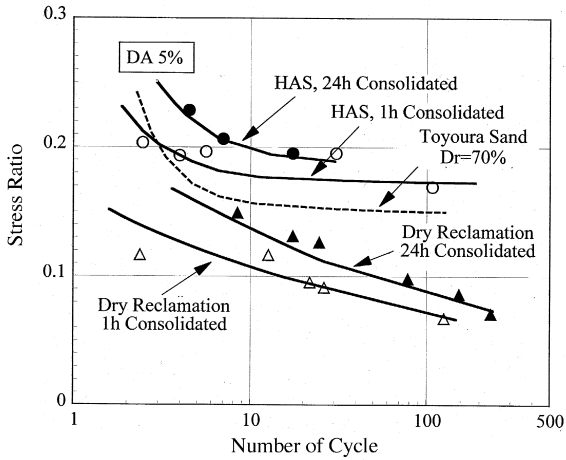

Fig. 14. Dynamic property of reclaimed fly ash.

liquefaction can be achieved by the slurry reclamation. On the other hand, the dry reclaimed sample shows a lower dynamic strength. Strength development is also confirmed in both types of reclamation samples (Fig. 14).

3. Man-made island construction using fly ash slurry

3.1. Outline

Man-made islands 100 m in diameter are often made in the construction of bridges. In conventional methods, such man-made islands are constructed by filling sandy soils into a steel pile cofferdamed area; however, the following problems have frequently been encountered:

1. Sliding failures of the seabed induced by the load of the fill.
2. Insufficient strength of the fill for subsequent construction work.
3. A large displacement of the cofferdam wall caused by lateral earth pressure exerted by the fill.

All these problems relate to the high density and low strength of the fill. Therefore they can be avoided by improving the filling method. For example, problem (1) can be solved by using a lower density material. Problem (2) can be solved by providing a self-hardening property to the fill. Problem (3) is alleviated by decreasing fill density and/or filling a self-hardening material in layers, as shown in Fig. 15 where submerged density of 0.6 g/cm^3 slurry and 0.8 g/cm^3 sand are compared. For a solution to these problems, our experience points in the direction of underwater placement using a light

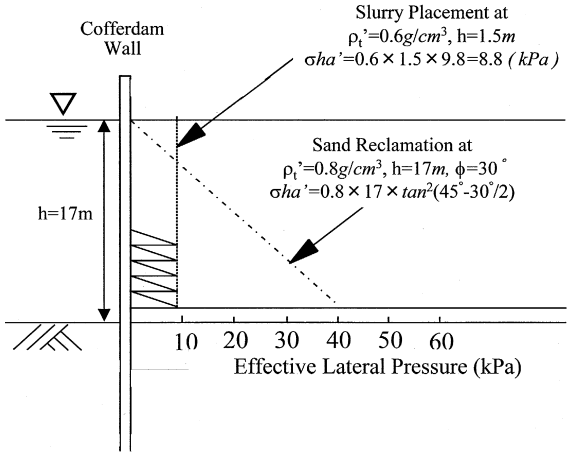

Fig. 15. Lateral pressures of reclamation methods.

and self-hardening material as the fill. However, this new idea differs considerably from conventional filling methods and there is no precedent in actual construction projects.

Coal fly ash slurry appears to be a good component for the slurry, due to the following properties: (1) lower specific gravity, (2) higher pozzolanic activity, and (3) spherical shape of particles. Property (1) provides the convenience of light weight. Property (2) is valuable for strength enhancement with cement addition [2,3,20]. And property (3) contributes to good pumpability. In some projects, fly ash/cement slurries have actually been used for grouting [1,21]; however, fundamental information, including relationship between strength development and composition of the slurry, its triaxial strength and applicability for underwater placement, has not yet been reported on.

The Hakucho Ohashi (The Muroran Bay Bridge), is being built in Hokkaido. The foundations of the two main towers are being built on 67-m diameter man-made islands made on the soft seabed. For the construction of these man-made islands, a new filling method consisting of underwater placement of self-hardening lightweight slurry into a cofferdamed area was applied instead of the conventional sandy soil filler. The authors carried out a series of studies to confirm the practicality of underwater placement of the fly ash slurries and to determine the optimal slurry composition.

3.2. Laboratory experiments

3.2.1. Procedures

3.2.1.1. Materials. Fly ash: Table 3 shows properties of fly ashes used. Fly ash AA was from Japanese coal and the others were from several types of Australian coal. Since the storage period after humidifying was $X < Y < Z$, their rank in terms of strength development could be expected to be $X > Y > Z$. Fly ash AA contained a smaller amount of calcium, so it was less suited as a slurry component.

Table 3
Properties of fly ashes and volcanic ashes

		Fly ash				Volcanic ash	
		X	Y	Z	AA	X	Y
Specific gravity		2.35	2.26	2.29	2.32	2.59	2.51
Mean diameter (μm)		80	27	50	27	290	530
Ignition loss (%)		7.0	5.7	5.5	3.1	–	–
pH		12.3	11.8	11.4	12.0	–	–
Chemical components (%)	SiO_2	55.6	54.6	55.8	59.2	–	–
	Al_2O_3	20.4	22.7	21.8	23.8	–	–
	Fe_2O_3	3.50	4.04	3.59	4.96	–	–
	CaO	6.58	6.33	5.91	4.33	–	–
Period after humidified		1 week	1 month	1 year	1 week	–	–

Cement: OPC was added for strength enhancement to the slurry.

Volcanic Ashes (VA): Two sandy volcanic ashes were used as a partial substitute material for fly ash, because of their high pozzolanic activity and light weight.

Water: Natural seawater from Tokyo Bay or an artificial seawater were used for mixing and curing.

3.2.1.2. Test procedures. Slurries were prepared by the single-mixing method as shown in Fig. 2. Terms for the slurry composition are defined as follows:

$$\text{volcanic ash content: } Ak = Wv/(Wv + Wa)$$
$$\text{cement content: } Ac = Wc/(Wv + Wa)$$
$$\text{initial water content: } Aw = Ww/(Wv + Wa + Wc)$$

where W_v, W_a, W_c and W_w are weight of dry volcanic ash, dry fly ash, cement and the seawater, respectively.

3.2.2. Lab test results

Since the slurry should be placed underwater, its viscosity is the first consideration when determining the composition of the slurry. Volcanic ash content is related to bleeding rate and contraction rate. As shown in Fig. 16, increasing A_k up to 65% increases segregation of the slurry. Segregation produces free water in the slurry and increases slump, but excessive segregation may cause blockage of pipelines during pumping. Since bleeding rate less than 3% would be safe for the trouble prevention, the volcanic ash content below 40% is suitable.

The fluidity varies considerably with the type of fly ash; it is necessary to determine the water content required for each fly ash slurry in laboratory tests before the actual filling work. Typical strength development of the slurry is shown in Fig. 17, and it can be seen that the slurries develop their strength immediately after preparation. When we

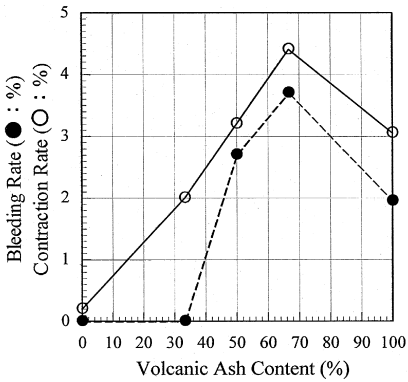

Fig. 16. Effect of volcanic ash content on slurry segregation (FA:Y; VA:X; $A_w = 50\%$, $A_c = 2\%$).

place a 1.5 m layer of slurry at 10-day intervals, 9 kPa of vertical load will be applied to the lower layers. According to Jaeger's equation [22], the critical load for lateral flow equals the quadruple of cohesion (C); therefore, the placed slurry must develop more than 2 kPa cohesion before the next layer is placed. Considering that C is equal to half of qu, the slurries in Fig. 17 develop 4 kPa qu within several hours after slurry preparation. We can, therefore, expect that the lateral pressure developed during placing will not increase after several hours in the same manner as Fig. 15.

In general, hardened slurry strength is dependent on both cement content and void ratio. As shown in Fig. 18, cement-free fly ash slurry develops a low strength. Since fly ash X contains 6% calcium, slurries made of fly ash Y have the potential for strength development of more than 200 kPa without any cement addition [4]; however, this self-hardening potential is likely to decrease as a result of hydration. Cement addition is very effective in strength enhancement, especially when cement content is above 2%.

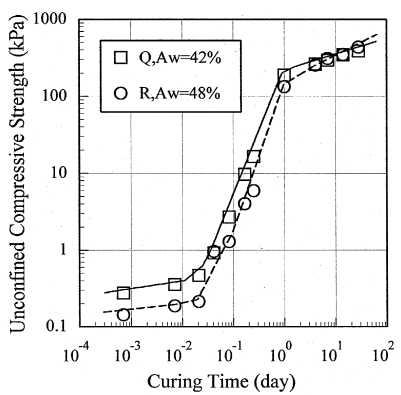

Fig. 17. Strength development of slurries (VA:X; $A_k = 30\%$, $A_c = 3\%$).

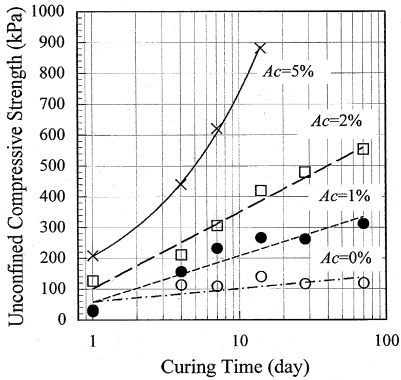

Fig. 18. Strength development of slurries (FA:Y; $A_k = 0\%$, $A_w = 50\%$).

Fig. 19 shows the relationship between strength and void ratio, where the following tendencies are seen;

1. The smaller the void ratio, the higher the strength.
2. The higher the fly ash content, the higher the strength.

Generally speaking, pozzolanic activity of volcanic ash is higher than that of usual fine aggregates. From Fig. 19, it can be confirmed that even the wet stored fly ash has a higher pozzolanic activity than the volcanic ash; therefore, we could use disposed fly ashes as a slurry resource if there were no legal restrictions.

The man-made islands were planned to be constructed over a year. Since the temperature of seawater in winter reaches 5°C, strength decrease caused by the lower curing temperature should be taken into account. The effect of temperature on strength is

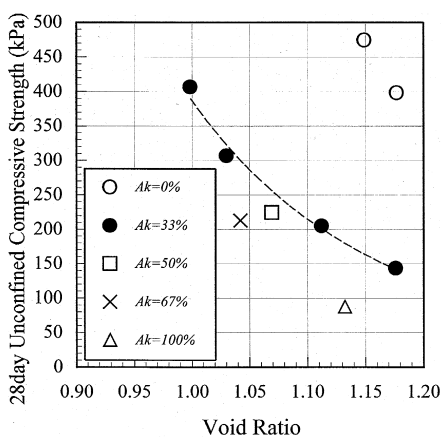

Fig. 19. Strength and void ratio of slurries (FA:Y; VA:X; $A_c = 2\%$, $t = 28$ days).

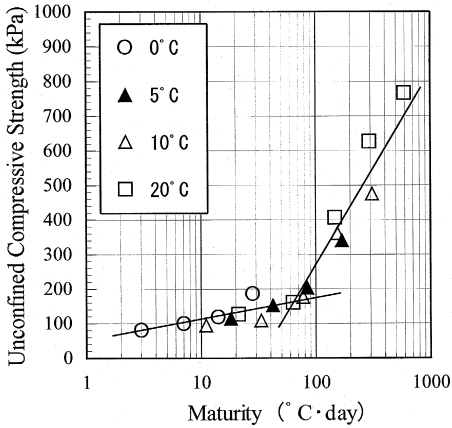

Fig. 20. Effect of curing temperature on strength (FA:X; VA:Y; $A_k = 30\%$, $A_c = 3\%$).

shown in Fig. 20 using maturity R($R = (T + 1)t$, where T is temperature in Celsius and t is time in days). Strength development, though depressed by lowering temperature, does take place below 5°C. The effect of curing temperature can be clearly expressed by R. Other laboratory tests in this project showed that a temperature decrease from 20°C to 5°C caused a decrease of 74 kPa cohesion, 190 kPa qu. As shown in Fig. 18, strength can be boosted by cement increase. This 190 kPa qu can be compensated for by a 1–2% increase in cement content, and hence, we can use fly ash slurry even at low temperatures.

3.3. Filling work in the Hakucho Ohashi project

3.3.1. Specifications for slurry placement

3.3.1.1. Composition and properties of the slurry. The composition of the slurry was fly ash, volcanic ash, OPC and seawater. Humidified fly ashes were transported by truck in 2.5 m^3 bags from the Tomato–Azuma power plant (Hokkaido Electric Power) located 100 km from the construction site. A finer volcanic ash, 0.29 mm mean diameter, was used as a partial substitute for fly ash and included as 30% of the volcanic ash content. OPC was used for strength enhancement of the slurry. The seawater in the cofferdamed pond was used as the mixing water.

Quality specifications of the slurry were: (1) slump: 11 cm (8–13 cm); (2) bleeding rate: 0–3%.

The strength requirement of the fill after 90 days is 100 kPa in cohesion (Cu), which corresponds to 260 kPa in unconfined compressive strength according to results of a series of triaxial tests. Since it seemed that there were many factors which could negatively influence the strength, such as a large variation in fly ash properties and the qu/Cu ratio of the slurry or decrease of density due to mixing with the seawater during the placement, a slurry composition was determined so as to develop cohesion of 320 kPa, which corresponds to 840 kPa in unconfined compressive strength in the laboratory

Table 4
Specifications of fly ash slurry

Fly ash	Cement content (%)	Initial water content (%)	Mixing time (s)	
			Range	Average
MO	5	35	74–89	79
UL	5	40	66–112	84
PK	5	40	66–90	75
DA	5	35	73–93	78
GSEH	5	45	54–111	70
WA	4	40	62–144	71
LI	4	40	61–86	69
CV	4	50	66–159	83
CV/BA	5	35	64–85	73
CV/EB	5	60	70–143	91
CV/H/BA	4	55	76–82	78
Cv/BA/IP	4	55	67–126	74
UL/BA(1)	5	40	66–123	76
UL/BA(2)	5	50	66–80	70
WA/GSEH	5	45	70–86	74

test. Because the properties of the slurry differed greatly with the type of fly ash used, the optimal composition for each type of fly ash was determined as listed in Table 4 through laboratory tests.

3.3.1.2. Machines for mixing and placing. Machines and apparatus used in this filling work are schematically shown in Fig. 21. Water content of fly ash and the volcanic ash were measured to adjust the water content of the slurries using an infrared moisturemeter [23]. A 2 m^3 forced action batch mixer was used for the slurry preparation. Because

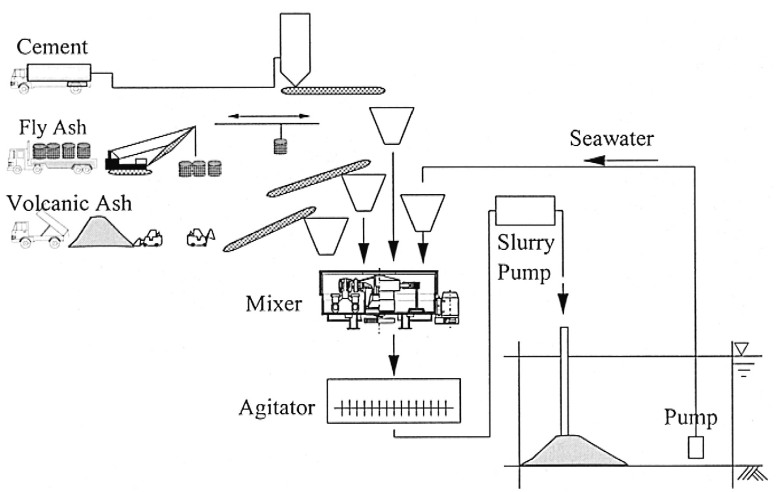

Fig. 21. Machines and apparatus used in filling work.

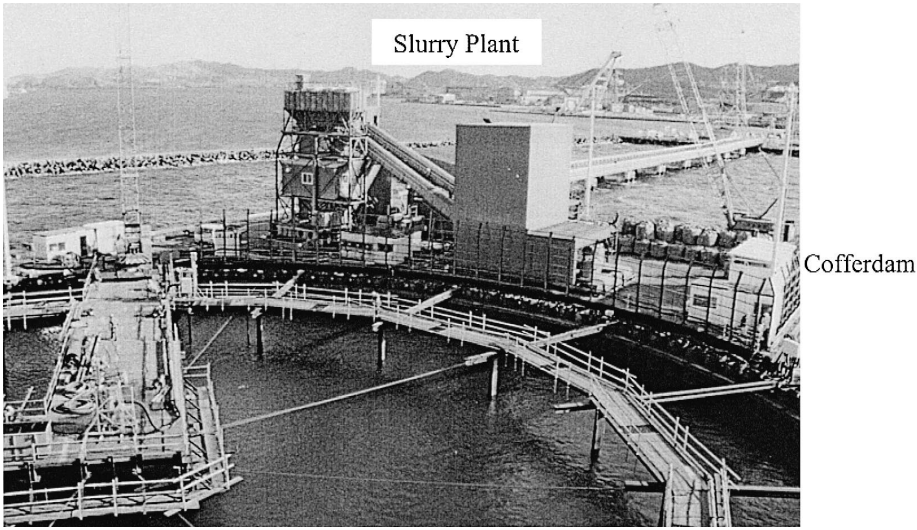

Fig. 22. Cofferdam and slurry plant.

the time required for homogeneous mixing depended on the type of fly ash used, the mixing time varied from 54 to 144 s as listed in Table 4.

Seventeen slurry placing points were determined by a field placing test, and the slurry was placed at three or four points daily. From the 22nd of October 1988 to the 16th of January 1989, 53,600 m^3 of slurry were placed into one of the two ponds enclosed by cofferdam, constructed of 1.3 m diameter steel pipe piles. For preparing 53,600 m^3 of the slurry, 46.1 Gg of wet fly ash, 22.2 Gg of volcanic ash, 2.6 Gg of cement and 14.2 Gg of the seawater were used. Fig. 22 shows the view of cofferdam and mixing plant.

3.3.2. Results of measurements

3.3.2.1. Mixing and transportation of the slurry. Properties of the slurry are shown in Table 5 and Fig. 23. There were large variations in slurry properties resulting from variations in the quality of the fly ash used. Slurries using the same type of fly ash have less variation in properties. The slurry quality can be controlled more precisely by

Table 5
Specifications and properties of slurry prepared

Properties	Specification	Slurry prepared	
		Mean value	Standard deviation
Slump (cm)	8–13	10.3	0.69
Wet density (g/cm^3)	1.60	1.60	0.073
28 day qu (MPa)	0.62	0.94	0.22
90 day qu (MPa)	0.84	–	–
Bleeding ratio (%)	≦ 3	2.1	1.26

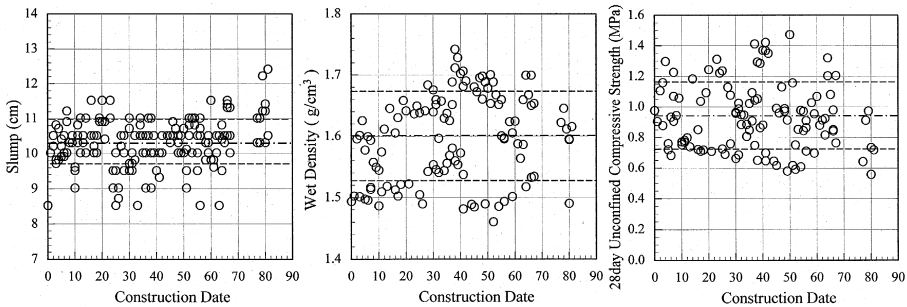

Fig. 23. Properties of slurry prepared. –·– Mean value, ––– Mean value ± std. deviation.

limiting the type of fly ash used. Throughout this filling work, no equipment failures nor pipeline blockages were experienced. Erosion of mechanical parts such as mixing blades or pipes was negligible, if anything.

3.3.2.2. Slope and temperature of placed mass. Shape and slope of the placed mass were measured daily during the filling work using a weight. The slope of each mass is plotted against the slump in Fig. 24, in which the correlation line of 6 m^3 tests in Fig. 10 is also shown. Though the correlation is not clear, the slopes are near to those recorded in placement tests using the 6 m^3 tank, as expected. The average slope of all the masses is 8.1°, and most slurry appears to have been placed without breakdowns of the slope.

Temperatures of the placed mass were measured at three depths, 6 m inside from the cofferdam wall, using thermocouples. In Fig. 25, the temperatures are plotted together with the depth of the fill, and both temperatures of the seawater and the atmosphere. Since slurry temperature was 10–20°C (mean value: 14°C), caused by the high temperature of the humidified fly ash, the sensors indicate a spontaneous increase in temperature just after contact with the slurry. The fill stayed at higher temperatures during the filling

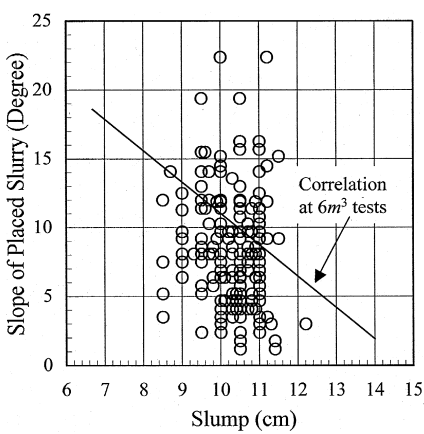

Fig. 24. Slope measured during placement.

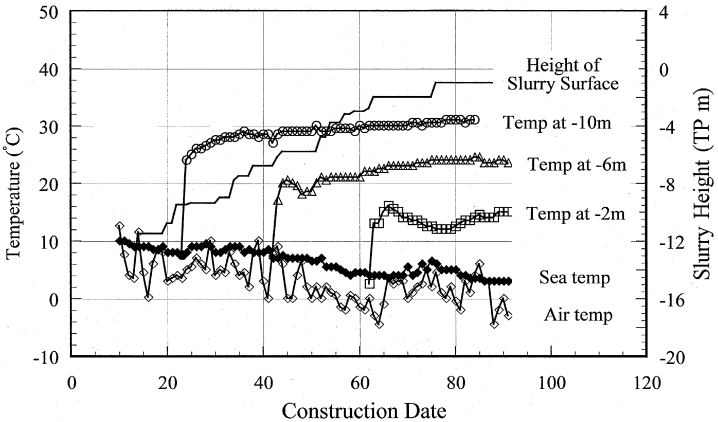

Fig. 25. Depth and temperarture of placed slurry.

work, while the temperature of the seawater continued to decrease. This higher temperature results from heat supplied from the initial heat of the slurry and hydration of the cement in the slurry.

Since most parts of the fill appear to stay above 10°C even in winter, inhibition of the strength development will be much less than what had been estimated.

3.3.2.3. Interaction of the cofferdam and placed slurry. To confirm the advantages of reduced effective lateral earth pressures on the cofferdam wall, the lateral pressures were measured during slurry placement. A typical change of the effective lateral pressures is shown in Fig. 26, in which the slurry surface depth change, determined using a ultrasonic density meter [24,25], is also plotted. The lateral pressure at −1.8 m began to increase just after the slurry reached the pressure cell, and increased up to 4 kPa at the

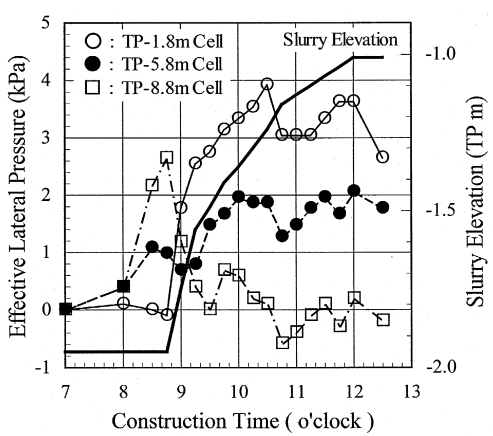

Fig. 26. Effective lateral pressure increase due to slurry placement.

end of the daily placement work. Since submerged density of the slurry used is 0.6 g/cm^3, the effective lateral pressure caused by the 0.94 m thickness is calculated as 5.64 kPa. This pressure is close to but slightly higher than the actual one. This difference may be due to the existence of a lower density slime layer, which might accumulate at the edge of the mass during placement, and would increase the height measured. The effective lateral pressures at deeper points are also plotted in Fig. 26. Since the slurry weight exerted pressure through the fill, the deeper the pressure cell was located, the quicker the lateral pressure increased. The lateral pressure increase diminished over time, because of a small elastic displacement of the cofferdam wall induced by the water level difference between the inside and outside of the cofferdam or due to the lateral pressure of the placed slurry itself.

Fig. 27 shows changes in the effective lateral pressures throughout the entire filling work. There were temporary increases; however, they did not remain and had no cumulative effect. The average lateral pressure is 3–10 kPa. The expected effective lateral earth pressure by the conventional method is 55 kPa; therefore, it can be reduced to 1/18–1/6 by using the new filling method.

Bending moments of the cofferdam wall were calculated from the measured stresses. As shown in Fig. 28, the moment increases with filling progress, however it did not exceed the designed maximum moment of 1.1 MN m throughout the filling work. In Fig. 28, a bending moment profile calculated for a sandy soil fill, with 1.8 g/cm^3 wet density and 25° internal friction angle, is also plotted to compare with the actual profile of the slurry filling. The maximum moment of the sandy soil fill is so large that it would be necessary to increase the stiffness of the cofferdam wall to prevent its rupture. On the other hand, slurry filling shows a lower moment of less than 1/5. In this figure, depth of the maximum moment in the slurry filling method is located at a greater depth than that in the conventional method using sandy soil fill. This difference in depth results from the cumulation of the bending moment in the slurry method. Displacement profiles of

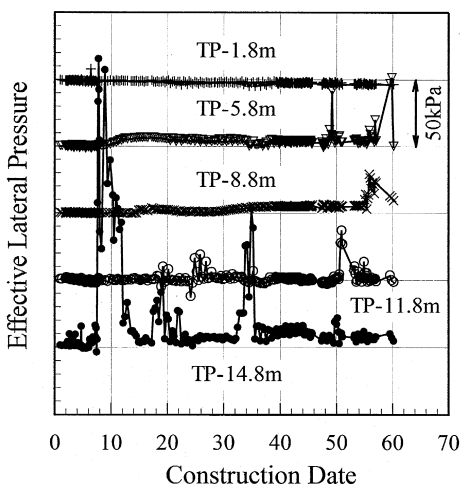

Fig. 27. Effective lateral pressure throughout filling.

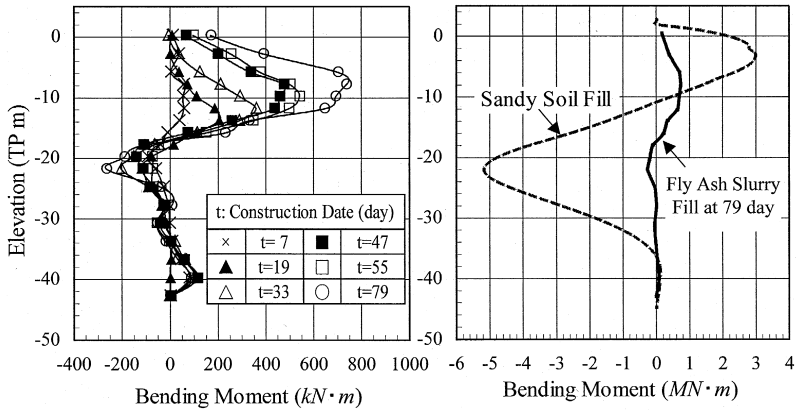

Fig. 28. Bending moment of cofferdam wall caused by filling works.

the cofferdam wall measured with a inclinometer are shown in Fig. 29. The displacement increased with filling progress, and reached a maximum value of 20 mm at the end of the filling work. If we fill with a sandy soil, one calculation shows 700 mm of displacement could be induced. Hence, the slurry filling method reduces displacement to 1/35 that of conventional method.

3.3.2.4. Properties of fill. One month after completing the filling work, the properties of the fill ground were checked at several points by both laboratory tests using boring samples and in-situ tests. Distributions of unconfined compressive strength and wet density are plotted in Fig. 30, and each property varies considerably with location. The variations result from differences in the slurry used, curing periods and curing tempera-

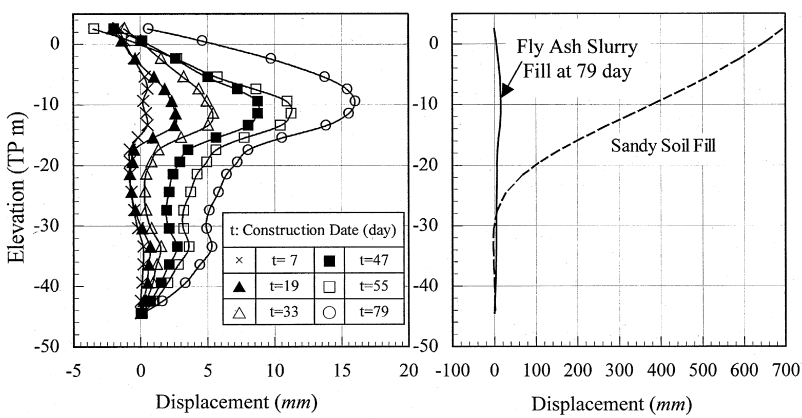

Fig. 29. Displacement profiles of cofferdam wall.

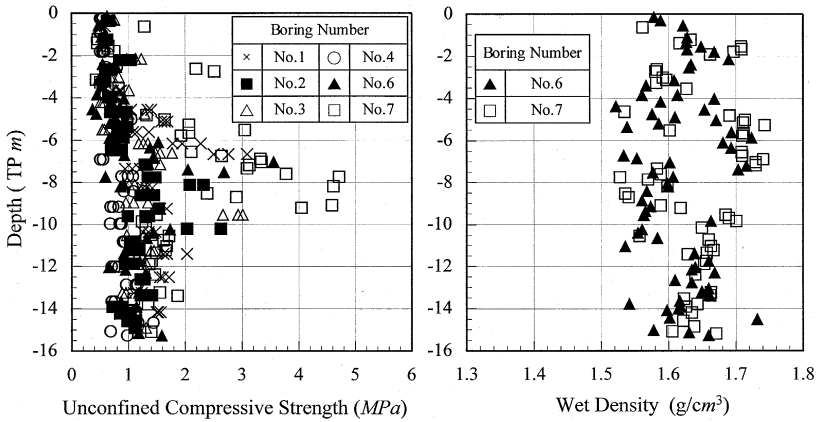

Fig. 30. Distribution of strength and wet density of fill.

tures. Fill properties are summarized in Table 6. For comparison with the mold samples, the estimated unconfined compressive strength (qu) of the boring samples at 28 and 90 days were calculated using the following equations;

$$qu_{28} = qu_t/(0.364\log(t) + 0.473),$$

$$qu_{90} = qu_t/(0.308\log(t) + 0.399),$$

where, qu_{28} and qu_{90}: qu at 28 and 90 days curing, qu_t: qu of a boring sample at t days curing.

In terms of the wet density, the boring samples exhibit a larger mean value and a smaller standard deviation than those obtained from the mold samples. This tendency results from the following;

1. The degree of both consolidation and segregation of the placed slurries was greater than those in the molds.
2. During the placing of the slurries, scarcely any mixing with the seawater occurred.

Table 6
Properties of fill

Properties	Specification for fill	Boring samples	
		Mean value	Std. deviation
Wet density (g/cm^3)	1.6	1.62	0.058
Dry density (g/cm^3)	–	1.14	0.087
Water content (%)	–	42.90	7.42
28-day qu (MPa)	–	1.06	0.61
90-day qu (MPa)	0.26	1.23	0.7
Elastic modulus (MPa)	–	359.7	256.3
Strain at failure (%)	–	0.81	0.29

As seen in Table 6, the fill's strength at 90 days is considerably greater than the specification, and is even greater than the slurry specification shown in Table 5. Comparing the strengths at 28 days curing, the boring sample shows a standard deviation three times as large, and a mean value 12% higher than the mold sample values. The large strength at TP-6–TP-10 m in Fig. 30 due to coal ash type used; i.e., coal ashes used from TP-6 to TP-10 m placement showed a larger potential for strength development with time. If it is required to lower strength standard deviation, controlling the coal ash type is important.

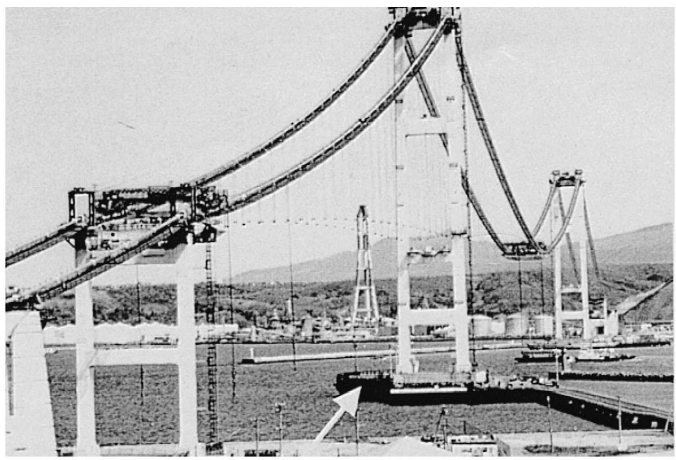

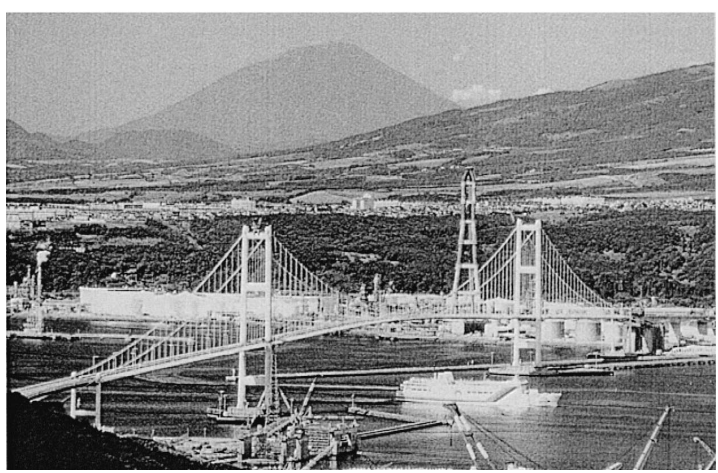

Fig. 31. The Hakucho Ohashi bridge and man-made island.

Seabed subsidence was measured during the filling. It reached 80 mm at the end of the filling, however the subsiding rate is so gradual and small that it did not affect the subsequent construction work.

Throughout the filling work, the following advantages of fly ash slurry reclamation were confirmed;

1. Even though different varieties of fly ash were used, the slurry could be prepared within the quality specifications by using appropriate equipment.
2. The new method reduces the lateral earth pressure to 1/18–1/6 that of the conventional sandy soil fill, and thus greatly reduces the bending moment and the displacement of the cofferdam wall.
3. In spite of filling work at low temperatures, the fill developed sufficient strength for subsequent construction work without requiring any soil improvement.

In this filling work, 46.1 Gg of fly ash was utilized. This new reclamation method can be used not only for island construction, but also for a variety of water-front project works.

3.3.2.5. Long-term stability of fill. All of the Hakucho Ohashi project was accomplished at May 1998. Fig. 31 shows the bridge together with the fly ash fill. Long-term properties of the fill were checked using samples collected at 11 depths during excavation inside of the fill. Table 7 shows the depth and slurry composition of the samples. The strength development is shown in Fig. 32, where a long-term increasing of the strength is seen for all the samples more than 10 years after filling work. Among the samples, slurries using CV type coal ash, which were used for placement at TP-6 to TP-10 m, increase strength larger than the others.

Table 7
Specification of long-term samples

Sample depth (m)	Mix design		
	Fly ash type	Cement (%)	Water (%)
0.5	LI	4	40
1.5	DA	5	35
2.5	DA	5	35
3.5	UL/BA	5	50
4.5	CV/EB	5	60
5.5	DA	5	35
7.0	CV	4	50
8.0	CV	4	50
9.0	CV/BA	5	35
10.5	CV	4	55
12.0	UL/BA(1)	5	40

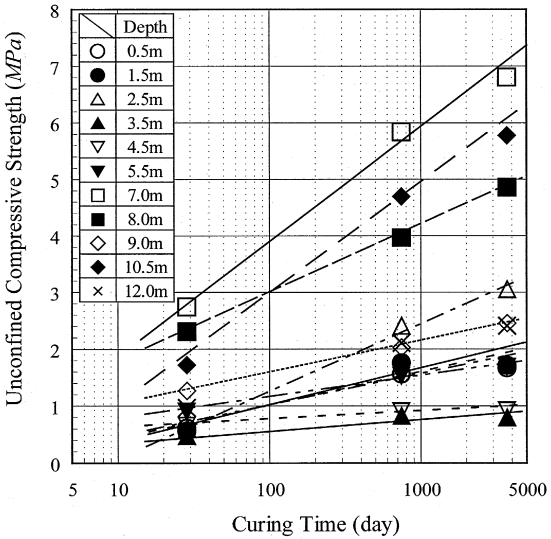

Fig. 32. Long-term strength of slurry fill.

Leaching tests were carried out using 10-year samples, and the results show a slight amount of Cr^{6+} leaching; however, all the leachates are within the concentration of Japanese environmental law.

4. Structural fill using lightweight slurry

4.1. Outline

In construction projects at soft alluvial and reclaimed area, light weight materials such as polystyrene foam (EPS) or air mortar are used for fill to prevent substantial subsoil large settlement. EPS has the merits of lighter density (0.01–0.03 g/cm^3) and sufficient ground strength (100 kPa),but has demerits on weakness against heat and organic solvents [26]. Air mortars, prepared by mixing foam with cement milk have a higher wet density of (0.5–0.8 g/cm^3) than EPS but are chemically stable and the strength can be adjusted by mix design [27]. The major merits of air mortars are easy preparation at the construction site, and superior fluidity.

Air mortar strength increases with density, but the density required is dependent on the circumstance. For structural fill use, wet density of 1.1 g/cm^3 is required. Air mortar having such density, however, seldom shows too much strength for easy re-excavation. Partial substitution of cement by coal fly ash would satisfy both the low strength and high density requirements. Mechanical properties including early strength, cohesion and creep have not been reported yet. Some of these properties have not been reported even for air mortars.

Table 8
Representative test samples of FAM

FAM no.	Compositions (kg/m^3, l/m^3 *)						Wet density (g/cm^3)
	Fly ash	OPC	VA	OFA2 *	Water *	Air *	
J-2	239	159	0	1.6	221	624	0.62
K-2	224	149	0	5.5	241	607	0.62
L-1	238	159	0	1.6	241	594	0.64
L-7	193	129	0	1.1	187	680	0.51
L-8	199	133	142	0.7	184	622	0.66
L-15	328	218	0	1.3	303	472	0.85
M-2	280	187	0	2.1	260	553	0.73
U-2	230	154	0	3.1	223	616	0.61
W-2	253	169	0	3.4	245	580	0.67

OPC: Ordinaly Portland Cement.
VA: Volcanic ash.
OFA2: Surfactant for foaming.

Since coal fly ash has a large surface area [28], a large amount of foaming agent would be absorbed on the surface, and would increase the amount of foaming agent required. Actual mix design, however, has not yet been reported. To confirm the unreported issues of fly ash-added air mortar (FAM), a series of laboratory tests were carried out. Then, FAM was applied as a structural fill around a high-rise building in Tokyo.

4.2. Experimental investigation

4.2.1. Materials and procedure

Fly ashes of quality below that for concrete additive (known as ''non-specification fly ash'') were used in the laboratory tests. Synthesized surfactant was used as a foaming agent. Volcanic ash was used for density adjustment and OPC was used for cement.

FAM was prepared by adding foam to fly ash/cement slurry. Wet density of the FAM was determined using a mud balance. Table 8 shows representative mixtures,

Table 9
Test specifications of FAM

Test name	Test specs	Curing dates for test
Unconfined compression	strain rate of 0.8%/min	1, 3, 7, 14, 28, 70, 91
Consolidation	standard oedometer test	28, 91
Creep	Unconfined compression at different creep load	91
CBR	Without immersion	28, 91
Triaxial compression	UU at 1.0%/min strain rate. Confined at 24.5, 49, 98, 196 kPa	28, 91
Dynamic compression	vertical load of 78 kPa and 157 kPa at 1.0 Hz for 100,000 s. Confined at 49 kPa.	28

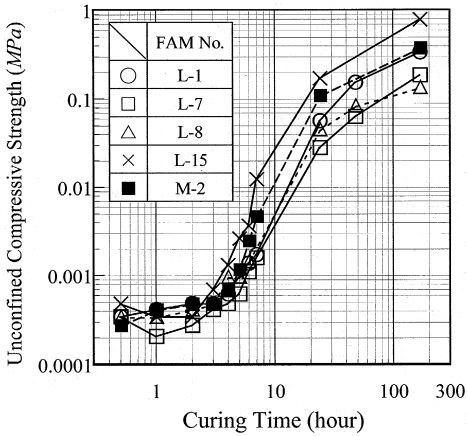

Fig. 33. Early strength development of FAM.

where quantity of foaming agent required varied with fly ash type. Test samples for CBR were prepared by pouring slurry into a 15 cm (ϕ) × 15 cm (h) mold.

Mechanical properties of the FAM samples were determined by the conditions listed in Table 9. Water saturation of the samples was difficult to control, and caused mechanical property data scattering. All the samples were cured and tested without water immersion.

4.2.2. Results and discussion

Early strength development of FAM is shown in Fig. 33, where a large increase in strength is seen between 3 and 24 h. Early strength is essential for planning actual filling work. For example, more than a 1-m lift of FAM can be filled the next morning since a 0.7 g/cm^3 wet density FAM develops enough strength to support a load of 7 g/cm^3 after 7 h, as expected in Fig. 33.

Fig. 34 shows typical results of unconfined compression test, where a large stress is sustained for over a large strain range. This large residual strength appears to be due to a

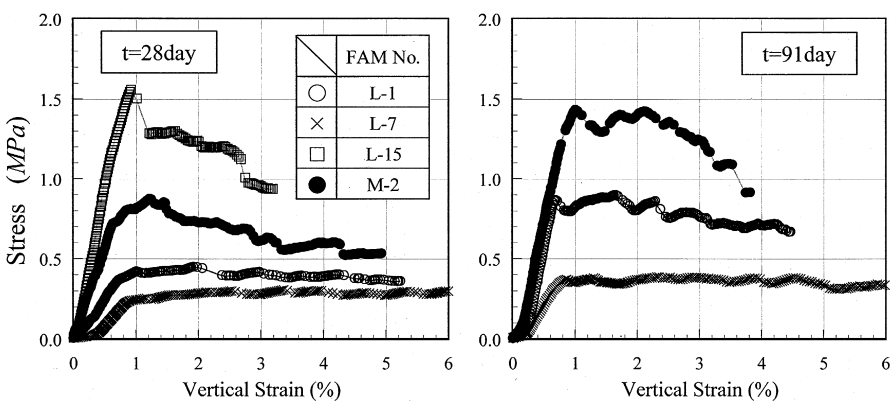

Fig. 34. Unconfined compression test results of FAM.

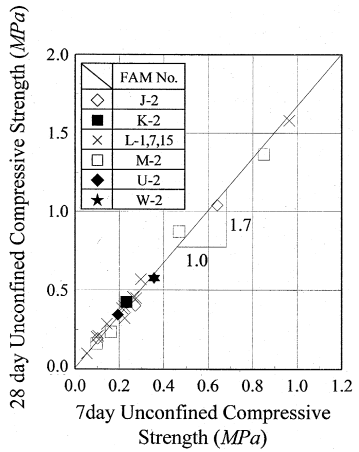

Fig. 35. Increase of FAM strength.

particular micro-structure of FAM composed of air bubbles with thin micro-walls. Broken micro-walls could form a rough failure plain, and shear stress could keep breaking the micro-walls into finer pieces. This could result in the high residual strength. This high residual strength is very effective in preventing a sudden failure of the fill, and should be taken into account in structural design.

Strength increase of FAM is shown in Fig. 35, where 28-day strength corresponds to 1.7 times 7-day strength. Various samples are plotted in Fig. 35; however, the relationship is constant.

Fig. 36 shows the relationship between unconfined compressive strength and dry density, in which L-8 etc. samples are mixtures using volcanic ash. Strength increases

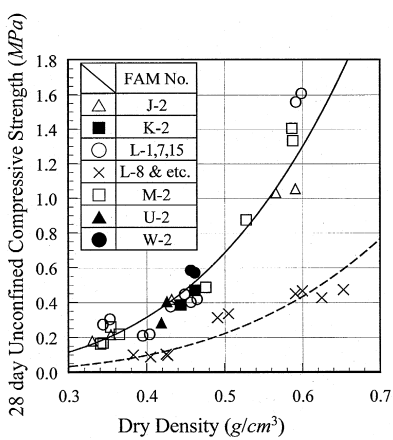

Fig. 36. Strength and dry density of FAM.

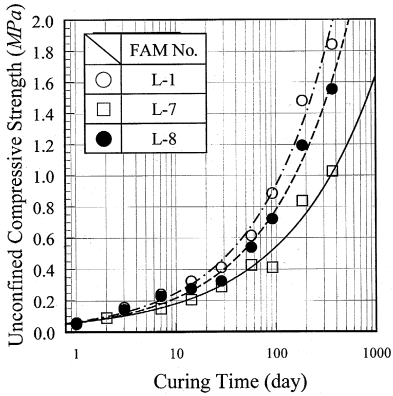

Fig. 37. Effect of A_k and A_c on strength.

with density increase in the same way as air-free slurries. Fly ash type has no effect on the relationship, but volcanic ash addition decreases strength. Strength can be expressed by dry density; however, wet density is much more important in field application because the stress exerted is dependent on wet density. Fig. 37 shows the strength of three FAMs using the same fly ash. As shown in Table 8, L-1 and L-8 have the same wet density, and L-8 is the sample of L-7 plus volcanic ash. Comparing L-1 with L-8, L-1 shows a slightly higher strength which could be caused by the difference in cement content. Dry density increased by volcanic ash addition does not affect strength, as seen in comparing L-7 to L-8. Together with the results in Fig. 36, volcanic ash can be recommended as a density-increasing material for FAM.

The relationship between fly ash cement ratio and 28-day strength is shown in Fig. 38, where increasing fly ash content has a minor effect on strength, and the effectiveness

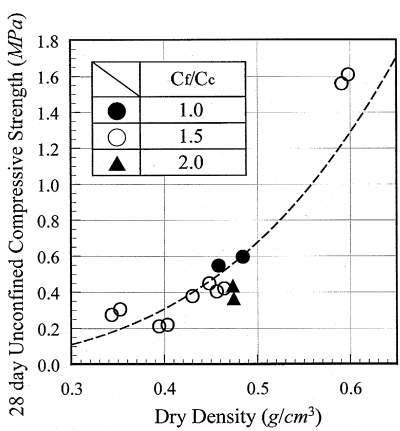

Fig. 38. Effect of fly ash/cement ratio (C_f / C_c) on strength.

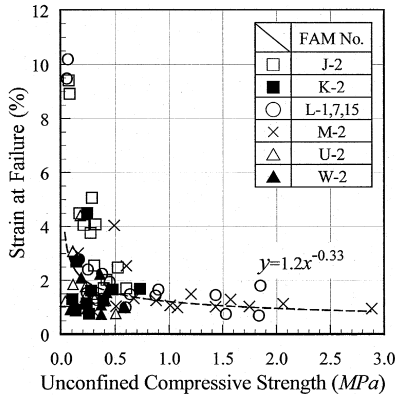

Fig. 39. Relationship between strength and strain at failure.

of fly ash substitution is confirmed. According to the tendency seen in Figs. 37 and 38, volcanic ash addition appears to be more effective in lowering strength than fly ash addition.

Fig. 39 shows the relationship between strength and strain at failure E_f. In the same way as with natural soils, strain at failure decreases with increasing strength, and fly ash type and mix-design have no effect on this relationship. For strength of more than 0.5 MPa, E_f of FAM is 1–2% on average.

In Fig. 40, examples of creep test results are shown. Creep load (P_{cr}) of 50% unconfined compressive strength causes a rapid strain increase leading to failure for L-7, but has no significant effect for L-15. It is important to predict the creep failure of FAM fill. Fig. 41 shows the relationship between the average strain rate, which is calculated by creep strain divided by elapsed time, and elapsed time. Since all the samples show

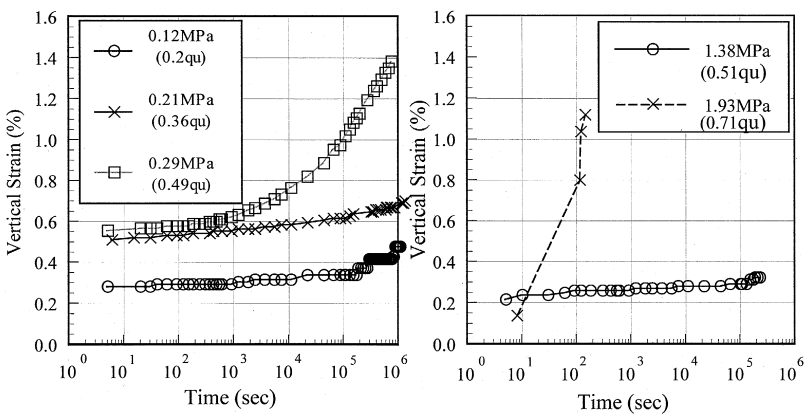

Fig. 40. Results of creep tests from 91-day (left: L-7, right: L-15).

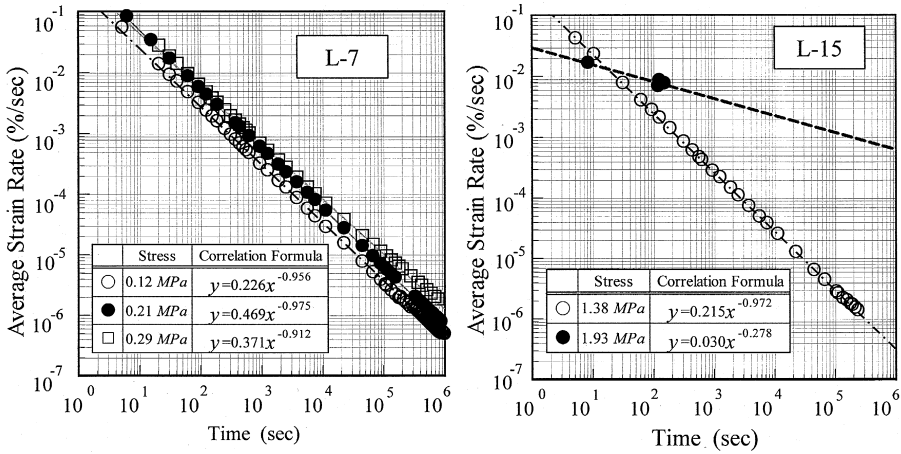

Fig. 41. Results of creep tests analyzed by average strain rate.

linear relationships, creep failure time can be estimated using rational hypothesis of creep failure at 1–2% in strain or E_f of unconfined compression test. Table 10 shows representative results of failure estimation for five types of FAM. From this table, it is concluded that FAM fill is safe against creep failure below the load less than 40% of qu.

Fig. 42 shows typical results of a series of triaxial compression tests. Stress steeply increases with strain, and remains at high level over a wide strain range, in the same way as unconfined compression tests. For natural soils, maximum stress is used for strength estimation; however, residual stress or averaged stress would be better in FAM to avoid overestimation of the strength caused by data scattering. From the result of triaxial tests, ratio of cohesion to qu is found to be 0.5.

Table 10
Failure time estimated from average strain rates

FAM no.	qu (MPa)	E_f (%)	Pcr (MPa)	Pcr/qu (%)	Time estimated for failure	
					Strain = 0% to E_f	Strain = 0% to 1%
L-1	0.88	1.52	0.11	12.5	1×10^{18} years	2×10^{14} years
			0.27	30.7	6×10^{61} years	5×10^{42} years
L-7	0.52	1.97	0.12	23.1	6×10^{13} years	1×10^{7} years
			0.21	40.4	2×10^{17} years	3×10^{5} years
			0.29	55.8	5.4 years	21.7 h
L-8	0.72	2.40	0.09	12.6	6×10^{18} years	7×10^{5} years
			0.22	30.7	2×10^{16} years	1370 years
L-15	2.71	1.14	1.38	51.0	2×10^{18} years	2×10^{16} years
			1.93	71.3	155 s	130 s
M-2	1.50	1.14	0.24	16.0	3×10^{10} years	2×10^{9} years
			0.61	40.8	2300 years	2.4 years

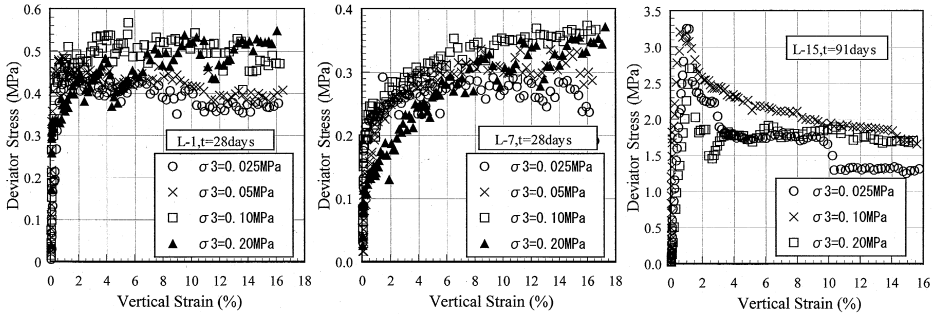

Fig. 42. Stress strain curves in triaxial tests of FAM.

4.3. Field observation

FAM was then applied as a structural fill around a high-rise building in downtown Tokyo. Fig. 43 shows FAM fill before and after surface covering. The quality of FAM and fill was sufficient for the demand of the specifications, and could depress temperature increase due to cement hydration by more than 20°C than conventional air mortar.

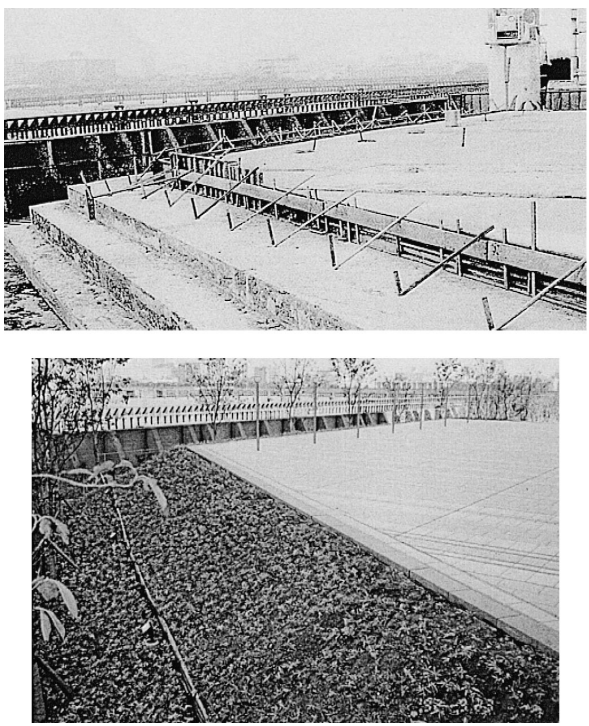

Fig. 43. Lightweight fill using FAM (left: FAM just after placement, right: final view after covering).

5. Conclusions

After researching the effective use of coal fly ash as fill materials, the authors reached the conclusion that fly ash slurry has a variety of merits both for utilization and sea disposal.

In Japan, a lot of marine projects are underway, including airport and harbor construction, and a vast amount of sandy soils are being used. Since land reclaimed using fly ash slurry has sufficient strength for land use and resisting liquefaction, attempts have been made to use fly ash slurry in many projects. Though at present large volumes are not utilized, advantages in slurry technology promise a slow but steady increase in utilization.

Acknowledgements

The authors would like to express grateful appreciation to the people involved in our projects.

References

[1] G.S. Littlejohn, Proc. 1st International Conf. on Ash Technology and Marketing, 1978, Paper 5.5.
[2] J.J. Funston, W.C. Krell, F.W. Zimmer, Civil Eng./ASCE (1984) 48–51, March.
[3] S. Horiuchi, K. Tamaoki, S. Goto, A. Onoue, Technical Research Report of Shimizu Corporation vol. 39 1984, pp. 1–9 (in Japanese).
[4] S. Horiuchi, TamaokiS. Goto, A. Onoue, Proceedings 7th International Ash Utilization Symposium, National Ash Association, USA, 1985, pp. 907–917.
[5] S. Horiuchi, M. Taketsuka, T. Odawara, H. Kawasaki, J. Mater. Eng., ASCE 4 (2) (1992) 117–133.
[6] S. Horiuchi, T. Odawara, T. Kusakari, K. Satoh, Technical research report of Shimizu corporation vol. 57 1993, pp. 1–9 (in Japanese).
[7] S. Horiuchi, K. Tamaoki, K. Yasuhara, Soils and foundations, Jpn. Geotechnical Soc. (Tokyo, Japan) 35 (1) (1995) 1–10.
[8] H. Kawasaki, S. Horiuchi, M. Akatsuka, S. Sano, J. Mater. Eng., ASCE 4 (2) (1992) 134–152.
[9] H. Shioya, S. Horiuchi, T. Furutani, S. Ooishi, Tsuchi-to-Kiso, Jpn. Geotechnical Soc. (Tokyo, Japan) 40 (12) (1992) 29–34 (in Japanese).
[10] K. Yasuhara, M. Hyodo, K. Hirao, Tsuchi-to-Kiso, Jpn. Soc. Soil Mech. Found. Eng. (Tokyo, Japan) 39 (2) (1991) 5–10 (in Japanese).
[11] K. Yasuhara, K. Satoh, M. Adachi, K. Kenkyo, S. Horiuchi, T. Kusakari, Technical Report of Ibaraki University, Hitachi, Japan 40 (1993) 41–52 (in Japanese).
[12] EPRI, Coal Ash Disposal Manual, FP-1259, 1979.
[13] J.A. Cunningham, R.G. Lukas, T.C. Anderson, Proc. of the Conf. on Geotechnical Practice for Disposal of Solid Waste Materials, 1977, pp. 227–245.
[14] K. Yasuhara, K. Hirao, T. S.Horiuchi, Technical Reports of the Geotechnical Research Institute, Nishinippon Institute of Technology (4) (1988) 17–26 (in Japanese).
[15] T. Sugimoto, I. Ohguchi, S. Horiuchi, Proc. 2nd Int. Symp. Environmental Geotechnology 1 (1989) 428–437.
[16] G.A. Leonards, B. Bailey, J. Geotechnical Eng., ASCE 108 (4) (1982) 517–531.
[17] H.B. Sutherland, T.W. Finlay, I.A. Cram, J. Institution Highway Eng. (1968) 19–27, June.
[18] G. Gatti, L. Tripiciano, Proc. 10th ICSMFE 2 (1982) 317–322.

[19] D.H. Gray, Y.K. Lin, J. Soil Mech. Found. Div., Proc. ASCE (1972) 361–380.
[20] H.W. Bradbury, Proceedings 5th International Ash Utilization Symposium (1979) 911–929.
[21] EPRI, Fly Ash Design Manual for Road and Site Applications, Vol.2: Slurried placement, CS-4419, 1986.
[22] J.C. Jaeger, Wiley, 1964.
[23] G.K. Brown, Ceram. Eng. Sci. Proc. 7 (11-12) (1986) 1245–1246.
[24] Sensall Instruction Manual, Sensall Instruments, 1987.
[25] S. Horiuchi, Y. Yasuda, Y. Ohtsuka, 17th Japan Nat. Conf. on Soil Mech. and Found. Engrg., The Japanese Geotechnical Society, Tokyo, Japan (1982) 1033–1036, (in Japanese).
[26] Y. Higuchi, Foundation Engineering and Equipment, Sogo-Doboku-Kenkyusho, Tokyo, Japan (12) (1990) 10–20 (in Japanese).
[27] T. Furutani, Tsuchi-To-Kiso, Jpn. Geotechnical Soc. (Tokyo, Japan) 37 (2) (1989) 73–77, (in Japanese).
[28] S. Mori, Fuji Techno-system, Tokyo, Japan, 1981, pp. 139–140, (in Japanese).